A Multi-Channel H_∞ Preview Control Approach to Load Alleviation Function Design

Ahmed Khalil and Nicolas Fezans

Abstract Gust load alleviation functions are mainly designed for two objectives: first, alleviating the structural loads resulting from turbulence or gust encounter, and hence reducing the structural fatigue and/or reducing the structural weight; and second, enhancing the ride qualities, and hence the passengers' comfort. Whilst load alleviation functions can improve both aspects, the designer will still need to make design tradeoffs between these two objectives and between various types and locations of the structural loads. The possible emergence of affordable and reliable remote wind sensor techniques (e.g. Doppler LIDAR) in the future also leads to consider new types of load alleviation functions as these sensors would permit to anticipate the near future gusts and other types of turbulence. In this paper, we propose a preview control design methodology for the design of a load alleviation function with such anticipation capabilities based on recent advancements on discrete-time reduced-order multi-channel H_∞ techniques. The methodology is illustrated on the DLR Discus-2c flexible sailplane model.

1 Introduction

Turbulence and gusts are causing dynamic variations of the aerodynamic forces and moments that are applied to the aircraft structure. In addition to causing structural loads that the structure should be designed to support, the resulting motion causes passengers discomfort and anxiety. Active load alleviation of turbulence and gust is not a new topic: the analysis, synthesis, design, and flight testing of an advanced

Ahmed Khalil

DLR (German Aerospace Center), Institute of Flight Systems, Lilienthalplatz 7, 38108 Braunschweig, Germany, e-mail: ahmed.khalil@dlr.de

Nicolas Fezans

DLR (German Aerospace Center), Institute of Flight Systems, Lilienthalplatz 7, 38108 Braunschweig, Germany, e-mail: nicolas.fezans@dlr.de

control system to alleviate gust loads and control structural modes of the Boeing B-52E during the Load Alleviation and Mode Stabilization (LAMS) program dates back fifty years [5]. Over the last decades, many gust load alleviation systems had been implemented on numerous airplanes, such as: Lockheed C-5A, Lockheed L-1011-500, Boeing B-1, Northrop Grumman B-2, Airbus A320, Airbus A330/A340, Airbus A380, Boeing 787, and Airbus A350 (see [23] and the references therein).

In [15] the authors synthesized an H_∞ optimal controller for alleviating the structural loads and enhancing the ride qualities of a flexible aircraft. In their work, the controller was synthesized by two different methods of the H_∞ optimal control: full-order based on the work of [6, 12], and fixed-structure based on the method presented in [2] and implemented in the MATLAB Robust Control Toolbox. For better anticipation of the future turbulence or gust, and hence better controller performance, feedforward and feedback load alleviation functions were designed together. The formulation of the feedforward load alleviation is made with a preview control problem formulation that is similar to the approach of [25], but in output feedback and adapted to a different application. Their simulation results showed that the structural loads and the normal load factor at pilot location (a ride quality index) had been greatly reduced compared to the case of no control (i.e., open loop) and also the to the case of feedback-only control. The same reduction had been successfully achieved by both the full-order and the fixed-structure H_∞ optimal control synthesis methods.

This paper extends the approach published in [15], where an explicit buffering of the preview signal was already made, to explicitly use the multi-channel capabilities provided by the structured H_∞ techniques. For conciseness reasons only a two-channel example is shown with a trade-off between a passenger comfort criterion and a structural loads criterion. The principles and ideas presented remain the same for more complex cases.

The paper contains two main parts: first the control design method is presented in a relatively generic way in Sect. 2 and an application to the design of a load alleviation function is presented in Sect. 3.

2 Using Preview Control for Gust Load Alleviation

In this work the optimal tuning of feedforward-enabled gust load alleviation controllers is investigated. The investigations shown in the present paper and in [15] are a continuation of the work published in [11, 8, 9] which focuses in optimizing the load alleviation controller(s). In [11, 8, 9, 10] the overall design problem for the Airbus XRF-1 configuration was presented. The algorithm for reconstructing the gusts and turbulence ahead of the aircraft based on Doppler LIDAR measurements was introduced in [11] and its performance was significantly improved in [10]. The feedforward parts of the load alleviation functions in [8, 9, 10] used a decomposition into several sub-functions based on time-frequency decompositions of the forthcoming turbulence and each of these sub-functions were fulfilled by

simple controllers which were tuned manually. Since each of these functions had a simple and well-defined task to perform, this manual tuning was easy for an experienced control designer. The work presented hereafter contributes to the development of more advanced and systematic control design methodologies for tuning either these sub-functions or the entire feedforward load alleviation function. Here the way multi-channel reduced-order H_∞ control design techniques can be used for synthesizing a combined preview-based feedforward and classical feedback gust load alleviation function is illustrated on a relatively simple example with only two channels. In practice in order to tackle industry-size control design problems a significantly larger number of channels would have to be defined, but the methodology would be the same as in the simple example shown hereafter.

2.1 Basics on H_∞ Control Techniques

This section provides a very short introduction to H_∞ control with the aim of easing the reading of the rest of the paper and by giving the non-specialist readers a general idea of these techniques even if this introduction can by no means nearly cover the extensive literature on H_∞ techniques. The concept of H_∞ control has been introduced in the late 1970's and early 1980's. The standard H_∞ problem formulation is illustrated in Fig. 1. This figure basically consists of a lower linear fractional transformation with the system/plant P last outputs $\boldsymbol{y}$ (measurements) being fed back to its last inputs $\boldsymbol{u}$ (control commands) through a controller K. The aim of the H_∞ control design is to find a controller K which minimizes the H_∞-norm $\|T_{\boldsymbol{w}\to\boldsymbol{z}}\|_\infty$ of the transfer function $T_{\boldsymbol{w}\to\boldsymbol{z}} = F_l(P,K)$ and provides a stable closed loop. The term H_∞ itself is derived from the corresponding Hardy space [29, 1] and can also be seen as a particular case of the L_2-induced norm for dynamic systems, if the dynamic system is linear.
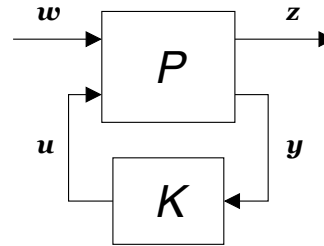

Fig. 1 Standard form for control synthesis

Controller synthesized with H_∞ techniques are often considered as "robust controller" due to the use of the H_∞-norm when applying the "small-gain theorem" to linear time-invariant (LTI) systems [29, 16, 1]. The basic idea of this theorem for the interconnection of Fig. 1 can be expressed as follows. Let $\gamma = \|T_{\boldsymbol{w}\to\boldsymbol{z}} = F_l(P,K)\|_\infty$, then the performance channel output $\boldsymbol{z}$ can be fed back to the performance chan-

nel inputs w through any system Δ such that $\|\Delta\|_\infty < 1/\gamma$ without destabilizing the closed loop $F_u(F_l(P,K),\Delta)$. As a consequence, if the performance channel inputs w and outputs z are chosen such that closing the loop from z to w can be interpreted physically as taking a meaningful set of uncertainties into account, then minimizing the H_∞-norm from w to z increases the robustness of the closed loop.

The small-gain theorem gives necessary and sufficient conditions for robust stability against unstructured uncertainties, but is often relatively conservative when dealing with structured uncertainties (no exploitation of the structure). In its basic formulation, it also provides no direct guaranty for robust performance in the presence of uncertainties (regardless of being structured or unstructured). Besides, the H_∞ control design algorithms are often used to shape the response or some transfer function of the closed loop. It is important to understand that in those cases the robustness of the closed loop is not necessarily increased and can even be significantly reduced. With other words, H_∞ techniques can be used to increase robustness, but the sole fact that H_∞ techniques have been used does not mean that the obtained closed loop is robust: the achieved performance and the physical meaning of the defined performance channel(s) must be analyzed to be able to conclude on robustness.

In this paper the H_∞ techniques are only used to specify the desired load alleviation behavior (i.e. to shape the gust/turbulence disturbance rejection) with and without preview of disturbance. The solutions obtained were found to be quite robust, but exhaustive robustness analysis as well as adding specific criteria to explicitly ensure robustness during the control synthesis are let for further work.

2.2 The H_∞ Optimal Control with Preview

In the present paper it is assumed (with no further discussion) that a sensor system is able to perfectly measure the vertical wind at some distance ahead of the aircraft and therefore that the vertical wind over a small time horizon in the future is known. The interested reader is referred to [11, 10, 13, 22] and the references therein for further information on the sensor technologies that could provide this capability.

In practice the sensor measures the wind at the current time but at a location that the aircraft has not reached yet. Even if, in the considered configuration, the measured wind is not expected to change significantly during the time the aircraft needs to reach the measurement location, it could theoretically change and the correct physical interpretation is that it is a remote measurement and not a glimpse into the future. Based on the remote wind information gathered ahead of the aircraft at the present time and in the past and based on the aircraft motion, a "best guess" on the future encountered wind/turbulence is made and used to anticipate and alleviate the resulting structural loads.

Preview control is a term that is found in the literature, see e.g. [4, 17, 18, 28, 25] and references therein, and which appears to be the most helpful search keyword for finding control design techniques for problems in which some reference or distur-

bance is "totally or partly known in advance". This very wide and inclusive definition of the term preview control is the one used here by the authors. Note that this simple definition is fully problem-oriented and not technique/algorithm-oriented at all. Note also that some applications of the so-called "model predictive control" (MPC) techniques are captured by this definition.

In the work presented in [15] the authors formulated the preview load alleviation problem as an H_∞ optimal control with preview. This formulation leads to the exact same problem structure as in various previous works on preview control, e.g. [25, 19], and the nomenclature used hereafter is chosen identical to the one used in [25]. A discrete-time state-space representation is preferred here due to the fact that it eases significantly the formulation of the time delays involved in the preview.

The steps to be followed to transform the bare system model into the discrete-time H_∞ preview control design plant are the following:

- Step 1: Build the (possibly nonlinear) continuous-time system model.
- Step 2: If not already defined in the original system model, add the previewed disturbance inputs into the model (without delay).
- Step 3: Trim the model at the desired operating point.
- Step 4: If necessary, linearize the model at the trim point from the previous step.
- Step 5: Define and integrate the performance channel(s) into the linearized model (integrate the required inputs and outputs as well as the corresponding weighting functions). Alternatively, the performance channel(s) could also be defined in the original model (before linearization).
- Step 6: Discretize the model with an adequate sampling time.
- Step 7: Add a chain of h unit delays, h being the considered preview time divided by the sampling time of the discrete-time model.
- Step 8: Proceed to the transformation steps that the specific control design method to be used may require (e.g. transformation into a "packed" system for MATLAB's `dhinflmi` or `dhinfric` functions or the "tunable generalized state-space" control design problem description expected by MATLAB's `hinfstruct` function).

The addition of delays for the preview input, see step 7, is detailed in Fig. 2. The discrete-time plant $G(z)$ contains the model of the system, with its performance channel from w to z, the control input u and the "regular" measurements y. It also contains an input d that is a signal which can be previewed over a number of h steps (for the chosen sampling time). The letter d was chosen here, as we are considering the preview of a disturbance (vertical wind) in the present work, but the future evolution of a reference might also be known slightly in advance (e.g. guidance commands passed to an inner-loop controller). d_p represents the measurement that is being taken at the current time and that (if perfectly measured and not changed in between) will become d after h time steps.

It should be noticed here that, unlike in many other works with preview control, the formulation of Fig. 2 includes an explicit buffering of the previewed input such that all the previewed input as well as its h previous values are explicitly passed to the controller. Theoretically, the controller states could be used to implement a

similar buffering strategy and control design algorithms would likely tend to provide such solutions, but with the risk of having this buffer functionality mixed with other dynamic elements in a controller state-space realization that would then become scarcely interpretable. Instead, the authors prefer a solution with this explicit and imposed buffering (as shown in Fig. 2) and the controller $K(z)$ to be a simple as possible and of low order.
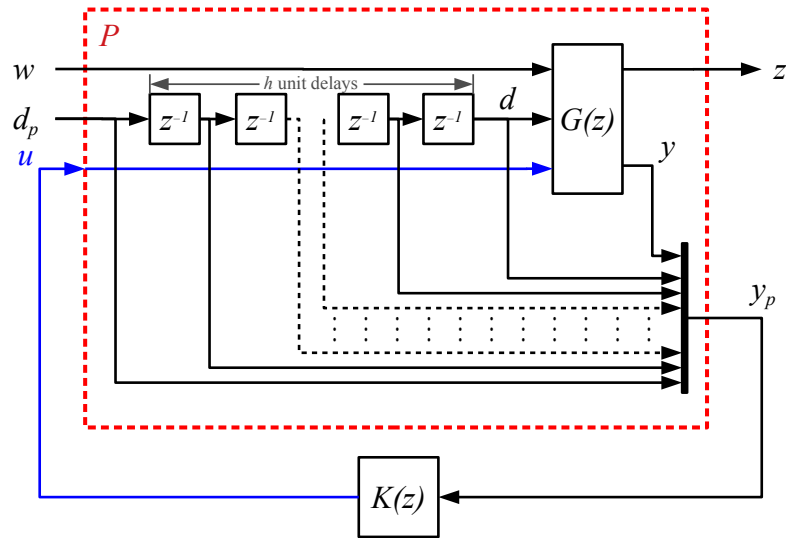

Fig. 2 Augmentation of the discrete-time H_∞ control design plant taking the previewed disturbance into account

Finally, depending on the exact use case, having separate preview inputs d_p and performance channel input w might not be necessary. For instance, in a pure disturbance rejection scheme the disturbance d_p will also be the input of the performance channel: the connection between w and $G(z)$ would then be removed and the performance channel is the transfer function from d_p to z. In another context, or in a multi-channel scheme, w could be another interesting physical input, e.g. another type of disturbance which can neither be measured nor be previewed but which should also be rejected by the closed loop. Similarly, various signals could be previewed and each could have a different preview horizon. As a consequence, Fig. 2 should be understood as a generic sketch of the different ways the original plant can be augmented for including preview signals rather than as the only augmentation considered hereafter. Later on, the system and control design criteria used are detailed along with the DLR's Discus-2c sailplane model.

2.3 Multi-Channel H_∞ Control Design

The H_∞ problems shown in the previous sections only included one performance channel from w to z. When working on multi-input multi-output (MIMO) systems or with various (usually conflicting) control design requirements, the "mono-channel" formulations force the designer to group the various degrees of freedom and criteria into one single transfer function with more inputs and outputs. In most cases, this approach has very significant drawbacks. The physical interpretation of the H_∞ norm of this transfer function is less direct or even becomes impossible. Besides, cross terms – which are usually uninteresting or even undesirable (from a control design perspective) – are introduced in the overall "cost function". For instance, in a problem where two single-input single-output (SISO) transfer functions (from w_1 to z_1 and from w_2 to z_2) are used to specify the desired behavior, the transfers from w_1 to z_2 and from w_2 to z_1 will necessarily be taken into account and steer the algorithm towards suboptimal or even undesirable solutions. The "classical" and mathematically efficient algorithms for solving H_∞ control design problems (e.g. [12]) are restricted to a single channel and additionally synthesize full-order controller (i.e. controllers with as many states as the plant).

To overcome these restrictions, many researchers have been investigating other approaches with the aim of permitting the synthesis of reduced-order controllers (less than the plant and possibly down to zero states) and with several independent performance channels. This currently remains a difficult problem to solve but some algorithms exist, some of which were integrated starting in 2011 in MATLAB's Robust Control Toolbox (in the `hinfstruct` function), which made them easily available. These algorithms are based on the work presented in [3, 2] and various other papers from the same authors. The suggested approach relies on non-smooth optimization techniques and a new multi-channel form is used. This form is illustrated in Fig. 3 with two channels. The gain β added to the first channel can be ignored here: it only plays a role later on for the considered application.

This formulation has the advantage of being very flexible. Each H_∞ channel is formulated based on a separate plant P_i and the controller K_i that must be designed can be fully independently specified (order, measurements, control commands). In practice, the plants P_i are often somehow related and the controllers K_i too but the control designer can freely select what they would like to express (no additional restriction in the method). Regardless of the choice of the control designers regarding the plants P_i and the constraints possibly imposed on the controllers K_i, the multi-channel control synthesis technique optimizes a program of the form given by Eq. (1), where $T_{w_i \to z_i} = F_l(P_i, K_i)$ is the closed-loop transfer function obtained by the lower linear fractional transformation of plant P_i and the controller K_i.

$$
\begin{aligned}
\text{minimize} \quad & \max_i \left\{ \left\| T_{w_i \to z_i} = F_l(P_i, K_i) \right\|_\infty \right\} \\
\text{subject to} \quad & \forall i, K_i \text{ stabilizes } P_i
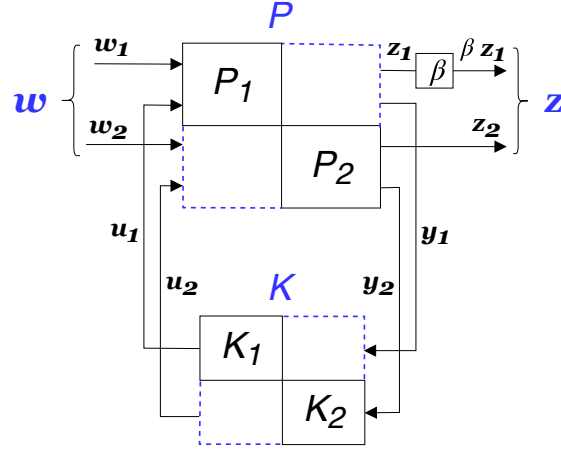\end{aligned}
\tag{1}
$$

Fig. 3 Standard form for multi-channel control synthesis

This flexible formulation can for instance be used to make a trade-off between various H_∞ requirements by selecting various different transfer functions for the same model: in this case the different plants P_1, P_2, etc. are basically representing the same bare dynamic system but with different performance channel input vectors w_i and output vectors z_i. Note that in that case the plants might contain states that are needed for some weighting functions in addition to the states of the bare system. When the same bare system is considered with different performance channels, additional constraints are set for the controllers K_i in order to ensure that they are equal: we are then looking for one unique controller that satisfies all the H_∞-criteria. This flexible formulation can also be used to perform robust control design by simultaneously considering several models (e.g. corresponding to various operating points or with different values for some uncertain parameters). This possibility is not used in the present work, but could be useful in some further work.

In the following the same basic model is used with different performance input and outputs vectors, but with the same control input vectors ($u_1 = u_2 = \dots$) and the same measurement output vectors ($y_1 = y_2 = \dots$), the multi-channel control synthesis problem can also be represented by the interconnection of Fig. 4. The designer can express their preferences in terms of trade-off between the channels by carefully selecting and introducing static/dynamic weighting functions on the inputs w_i and outputs z_i of the performance channels. Note that the inputs w_i and outputs z_i can be vectors and the transfer function $T_{w_i \to z_i}$ will have possibly several singular values. The obvious advantage of this multi-channel formulation, compared to considering the transfer $T_{[w_1, w_2, \dots]^T \to [z_1, z_2, \dots]^T}$ obtained by merging all performance channels, is that the cross transfer functions $T_{w_i \to z_j}$ with ($i \neq j$) are not part of the cost function to be minimized. In most control design problems these cross transfer functions make no sense for the control design problem.
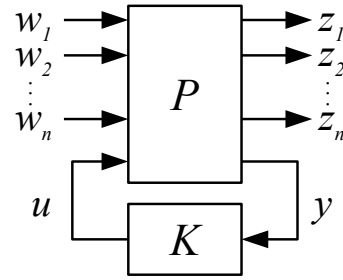
Fig. 4 Multi-channel single model and single controller control synthesis

2.4 Definition of the Performance Target Value(s)

Most control design tasks involve some trade-off between conflicting objectives and constraints. The control designers should understand the real constraints and needs of their application and the corresponding priorities between them. Eventually, they should translate them into well-defined mathematical objective or constraint functions, which can be provided to the control design algorithms. For the design of load alleviation function, the real objective is to enable a reduction of the overall weight, mainly through a reduction of the structure weight. In order to enable this weight reduction, the loads envelope – defined through the minimum and maximum loads occurring in all cases specified in the certification – must be reduced. Static and dynamic loads result from a large number of situations: gusts, maneuvers, landing, high-speed taxiing, pressurization, gyroscopic effects, etc. Consequently, a gust load alleviation function can lead to weight reduction only when the sizing cases result from gust loads. If, for example, the second highest loads are 10 % lower than the gust loads without load alleviation function, then gust load reductions up to 10 % correlates with potential weight savings. Beyond this value, weight savings can only be obtained if these second highest loads are also reduced. In addition, it is very often that gust load reductions at some locations (e.g. at wing root) will be obtained at the expense of gust load increase at some other locations (e.g. near the control surfaces used by the load alleviation function). Hence, a trade-off between the weight savings and penalties over the complete aircraft has to be made.

In order to ease the expression of the preferences, the various loads are usually normalized. This is necessary due to the fact that the orders of magnitude for the considered loads strongly differ (e.g. between wing root bending moments and the bending moment at the most outboard locations). The signals usually are not even of the same physical dimension (e.g. bending moment vs. shear force). A typical way of normalizing these loads is to divide them by their corresponding load envelope values. This leads to have loads above one for load increases and below one for load reductions.

After this normalization step, if all loads are to be reduced to 0.9 or less of their original values, then at least 10 % load reduction will be gained. Preferences between these loads are expressed by multiplying them by additional factors. By multiplying, for example, a particular load channel by a factor of 1/0.85 and an another

by a factor of 1/1.05, the designer can express that a reduction of 15 % is desired on the former load channel ($0.85 = 1 - 15\%$), and that in order to reach this performance an increase of 5 % can be tolerated on the latter ($1.05 = 1 + 5\%$). The control design algorithm will be configured such that a target performance of 1 is sought. If the algorithm could theoretically reach a better performance, it should not however be achieved. The underlying idea of this is that a controller which achieves a better performance than required will (in most cases) have a higher control activity. This is not desired because it increases the actuator load cycles, potentially increases the structural fatigue near the control surface, and might reduce the robustness margins, especially against unmodeled dynamics or delays. The desired load reduction or tolerable load increase for each channel are tuning parameters for the load alleviation function designer.

There are often additional performance margins that need be considered. Indeed, some effects might not be possible or easy to take into account such as uncertainties in the control design problem. These are for instance the errors in the gust and turbulence fields determined by a Doppler LIDAR sensor. The entire processing of such errors can be found in [11]. By looking closely at the results from [11], it can be observed that the error (between estimated and real wind profiles) made at each location and point in time is not independent. The overall wind reconstruction error depends on the buffering of the measurements, the noise on each individual measurement, and the Tikhonov regularization/smoothing method. Instead of attempting to take these errors (and their complex interdependencies) explicitly into account, the synthesis is performed under the assumption that the previewed wind information is perfect, but with an additional margin defined on the load alleviation performance requirements. For instance, if a 10 % alleviation performance is desired, then the control design will be made with a target of "10 % + margin" (say 14 %), and a perfect wind information will be assumed. The margin needs to be defined such that in practice the load alleviation performance obtained still reaches the desired 10 % when combining the designed load alleviation function and the imperfect wind information. Due to the complexity of the wind reconstruction errors, it might become necessary to determine the level of performance margin to be applied in an iterative way.

Even though it is not shown in the present paper, the trade-off between performance and robustness against model uncertainties (here in the aircraft model itself, and not in the wind reconstruction) is implicitly taken into account in the process described here. If model uncertainties need to be taken into account, this can be done through either an uncertainty block or a discrete set of models. The more the level of uncertainties to be taken into account, the higher the control activity in order to still reach the desired level of load alleviation performance in the worst case. For a very large level of uncertainties, the desired level of performance might not be achievable anymore, and in this case, the control design algorithm will stop before reaching the target value of 1.

3 Application to Gust Load Alleviation with Preview

3.1 Used Flexible Aircraft Model

3.1.1 DLR's Discus-2c Sailplane

Although this work is primarily intended to be applied to large transport aircraft (CS/Part 25 of the airworthiness standards), an aeroelastic model of a sailplane is used hereafter. The herein proposed method will be applied to the Generic Business Jet Aircraft model used in [20, 21], in which robust control techniques are used for feedback load alleviation, i.e. without the preview based on the Doppler LIDAR. The sailplane model used hereafter was chosen because it is readily available to both authors and is suited for gust load alleviation purposes. The model and the loads sensor calibration were derived from flight test using system identification and exhibited excellent match with the test data. The orders of magnitude in terms of loads and velocity are very different from the ones of a larger airplane, but the model structure as well as the relationships and coupling between states, inputs, and outputs are representative of those of a larger airplane.

The DLR's Discus-2c is shown in Fig. 5 and is a high-performance single-seat sailplane. The aircraft has the general mass and geometry characteristics given in Table 1. The aircraft is equipped with a flight test instrumentation which includes: a 5-hole probe nose boom, a GPS receiver, an INS platform, 46 strain gauge sensors and 15 three-axis accelerometers at different aircraft locations. Previous flight test campaigns provided the data enabling the development of a nonlinear aeroelastic model of the aircraft using system identification techniques (see [27, 26] and the references therein). This aeroelastic model allows for the calculation of the shear forces and torsional and bending moments at 7 different load stations: 6 per wing and 1 for the horizontal tail.
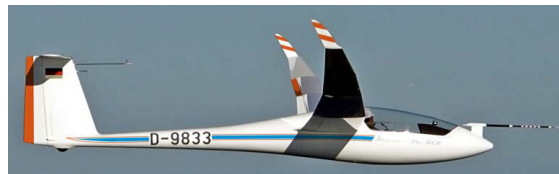

Fig. 5 DLR's Discus-2c sailplane in flight

In this work, only the symmetric motion and loads are considered; hence, only 3 load stations (WR1 / WR4 / WR6) and 5 accelerometers (WR4F / WR4R / WR7F / WR8F / WR8R) of the right wing semi-span, plus 1 accelerometer of the IMU (for ride qualities), will be considered, see Fig. 6. The horizontal tail loads and accelerometers will not be considered. For the rigid-body motion, only the short-period mode is considered; whereas for the flexible degrees of freedom, only the first and second wing vertical bending modes (see Table 2) are considered. Only symmetrical gusts and turbulence are considered hereafter, therefore only the following

12 Ahmed Khalil and Nicolas Fezans

Table 1 DLR's Discus-2c geometry and mass characteristics

Parameter	Value	Unit
Chord	0.685	m
Span	18	m
Wing area	11.39	m^2
m (with pilot 1 or 2)	451 or 422	kg
I_{xx}	3190	kg.m^2
I_{yy}	870	kg.m^2
I_{zz}	3900	kg.m^2
$I_{xy} = I_{yz} = I_{xz}$	0	kg.m^2

two control surfaces were kept in the model: the elevator on the horizontal tail with first-order actuator dynamics, and symmetric ailerons on the wing also with first-order actuator dynamics (different time constants). The ailerons of the real sailplane are mechanically connected and can only be deflected asymmetrically: the symmetrical aileron deflection capability only exists virtually in the simulation model. The model used in this work has 10 regulated output channels: 1 for normal load factor at pilot location (n_z^{pilot}, non-dimensional), 3 for shear force (SR1 / SR4 / SR6, in newtons), 3 for torsional moment (TR1 / TR4 / TR6, in newton-meters), and 3 for bending moment (BR1 / BR4 / BR6, in newton-meters).
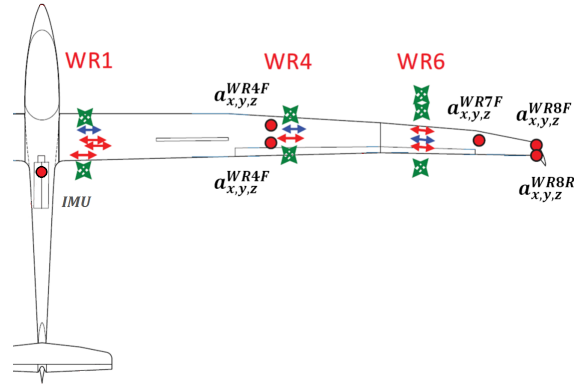

Fig. 6 DLR's Discus-2c load stations and distribution of measurement sensors (red circles: accelerometers)

3.1.2 Model Equations

The general equations of motion of a rigid aircraft can be expressed in the body axis system as in Eqs. (2), whereas Eqs. (3) represents the rigid-body kinematics equations, and finally the rate of change of the center of gravity (CG) position measured with respect to the inertial axis system is given by Eq. (4), see [7]. u_K, v_K and w_K are the components of the velocity vector of the CG relative to the inertial (New-

Copyright by the author(s) and/or respective owners. Published with authorisation by CEAS.

Table 2 DLR's Discus-2c modal characteristics (in vacuum)

	Mode	
Parameter	1	2
Description	1st wing vertical bending	2nd wing vertical bending
Generalized mass, kg.cm^2	20	10.35
Frequency, rad/s	16.02	48.59
Damping ratio	assumed 0	assumed 0

tonian) axis system (i.e., ground speed), p, q and r are the rotational velocities in body-axes, Φ, Θ and Ψ are the 3-2-1 Euler angles, x, y and z are the components of the position vector, X, Y and Z are the total external (aerodynamic + propulsive) forces, L, M and N are the total external (aerodynamic + propulsive) moments, m is the aircraft mass, g is the gravitational acceleration, and finally, $I_{..}$ are the aircraft moments and products of inertia around different axes (with "." being x, y or z). In Eqs. (5) the relation between (u, v and w), (u_K, v_K and w_K) and (u_W, v_W and w_W) is given, where u, v and w are the components of the velocity vector of the CG relative to the air (i.e., airspeed), whereas u_W, v_W and w_W are the components of the wind velocity vector relative to the inertial axis system.

$$
\begin{aligned}
m\left(\dot{u}_K + qw_K - rv_K\right) + mg\sin\Theta &= X \\
m\left(\dot{v}_K + ru_K - pw_K\right) - mg\cos\Theta\sin\Phi &= Y \\
m\left(\dot{w}_K + pv_K - qu_K\right) - mg\cos\Theta\cos\Phi &= Z \\
I_{xx}\dot{p} - I_{xy}\left(\dot{q} - pr\right) - I_{xz}\left(\dot{r} + pq\right) - I_{yz}\left(q^2 - r^2\right) + \left(I_{zz} - I_{yy}\right)qr &= L \\
I_{yy}\dot{q} - I_{xy}\left(\dot{p} + qr\right) - I_{yz}\left(\dot{r} - pq\right) + I_{xz}\left(p^2 - r^2\right) + \left(I_{xx} - I_{zz}\right)pr &= M \\
I_{zz}\dot{r} - I_{xz}\left(\dot{p} - qr\right) - I_{yz}\left(\dot{q} + pr\right) - I_{xy}\left(p^2 - q^2\right) + \left(I_{yy} - I_{xx}\right)pq &= N
\end{aligned}
\tag{2}
$$

$$
\begin{aligned}
\dot{\Phi} &= p + q\left(\sin\Phi\tan\Theta\right) + r\left(\cos\Phi\tan\Theta\right) \\
\dot{\Theta} &= q\cos\Phi - r\sin\Phi \\
\dot{\Psi} &= q\left(\sin\Phi\sec\Theta\right) + r\left(\cos\Phi\sec\Theta\right)
\end{aligned}
\tag{3}
$$

$$
\begin{bmatrix} \dot{x} \\ \dot{y} \\ \dot{z} \end{bmatrix} =
\begin{bmatrix} \cos\Psi & -\sin\Psi & 0 \\ \sin\Psi & \cos\Psi & 0 \\ 0 & 0 & 1 \end{bmatrix}
\begin{bmatrix} \cos\Theta & 0 & \sin\Theta \\ 0 & 1 & 0 \\ -\sin\Theta & 0 & \cos\Theta \end{bmatrix}
\begin{bmatrix} 1 & 0 & 0 \\ 0 & \cos\Phi & -\sin\Phi \\ 0 & \sin\Phi & \cos\Phi \end{bmatrix}
\begin{bmatrix} u_K \\ v_K \\ w_K \end{bmatrix}
\tag{4}
$$

$$u = u_K - u_W$$
$$v = v_K - v_W$$
$$w = w_K - w_W \qquad (5)$$

By using the concept of a lumped-mass vibration structure, the total elastic displacement of that structure expressed in the structural reference axis system might be expressed in terms of modal expansion using n free-vibration modes as in Eq. (6), where d_E is the total elastic deformation, ϕ_i is the vibration mode shape (eigenfunction), η_i is the generalized coordinate associated with the ith vibration mode.

$$d_E(x,y,z,t) = \sum_{i=1}^{n} \phi_i(x,y,z)\,\eta_i(t) \qquad (6)$$

These n generalized coordinates are governed by the n equations given by Eq. (7), where ζ_i and ω_i are the modal damping and natural frequency, respectively, whereas m_i and Q_i are the generalized mass and force, respectively, each associated with the ith vibration mode.

$$\ddot{\eta}_i + 2\zeta_i\omega_i\dot{\eta}_i + \omega_i^2\eta_i = \frac{Q_i}{m_i}, \qquad i = 1,2,\cdots,n \qquad (7)$$

By using the mean axis system (one at which the relative translational and angular momenta about the center of mass resulting from elastic deformation of a structure undergoing free vibration diminish at every instant), see [24], an aeroelastic model is constituted of Eqs. (2, 3, 4 and 7). These equations are 12+n in number, have 12+2n states, and are nonlinear and coupled differential equations of first and second order.

To complete the aeroelastic model, expressions for the external forces and moments and the generalized forces are needed (aerodynamic model). The aerodynamic model used in this work is expressed via partial derivatives (aerodynamic transfer functions) of the motion variables, control surface inputs, and the flexible degrees of freedom of the aircraft. For the example aircraft used for the simulation in this work, these derivatives had been obtained by system identification from flight tests (see [27, 26]).

These 12+n nonlinear differential equations can then be solved for trim at a given steady flight condition. After solving the trim problem, they can be dissolved into steady equations plus small perturbations (linear differential equations) added to them. The resulting linear differential equations (in state-space form) will then be used for the control synthesis as will be seen in the next sections, see [14].

For all the results presented hereafter the chosen flight point is defined by a steady rectilinear flight with a true airspeed $V_{TAS} = 160$ km/h and an altitude $H = 3000$ m (with standard atmospheric conditions). On the sailplane, the only varying mass (for weight and balance) is the pilot himself. The weight and balance parameters are given in Table 1 and the mass of pilot #1 was taken. The sampling time used for the discrete-time system is always 10 ms in the work presented in this paper.

3.2 Control Design Problem

In this application, two H_∞ performance channels were defined. For both channels the vertical wind is the only input. The output of the first performance channel is the variation of the vertical load factor at the pilot's location. The output of the second performance channel is the vector of the following 9 normalized load variations (Δ BR1, Δ SR1, Δ TR1, Δ BR4, Δ SR4, Δ TR4, Δ BR6, Δ SR6, Δ TR6) – compared to the trim loads – that are defined on page 12. In addition to the disturbance measurement and preview, the IMU measurements as well as the measurements from several accelerometers on the structure are considered.

In order to illustrate the trade-off that can be made between the vertical load factor at the pilot's location (which can be understood as a passenger comfort criterion) and the structural loads, a weighting factor β is introduced on the n_z output (output of the first performance channel, see Fig. 3). Increasing β increases the importance given to the passenger comfort compared to the structural loads.

The results shown hereafter are based on two different formulations. The first one is based on a single channel formulation with the two aforementioned channels merged into one single channel (with $\beta = 1$) and solved with both a full-order technique (using MATLAB's `hinfsyn` function) and with a reduced-order nonsmooth optimization-based technique (using MATLAB's `hinfstruct` function). This formulation permits to compare both techniques on a common example. The second formulation is the actual multi-channel as described earlier, and which can only be solved with the latter technique.

3.3 Results

First, the results provided by both techniques for the single-channel problem are compared. In the case of full-order discrete-time H_∞ optimal control, it can be seen from Fig. 7 that the H_∞ norm decreases from 1.07 for the feedback-only case to 0.96 when a zero-preview feedforward loop is added. After that, it decreases monotonically with increasing preview length (or preview time) until reaching a lowest value of 0.68 at a preview length of 18 (or a preview time of 0.18 s with the sampling time of 10 ms used). After reaching this lowest value, no more performance enhancement could be obtained even with increasing the preview length. In Fig. 9, this enhancement in the H_∞ norm could be seen as a reduction in the maximum absolute values of the regulated outputs. The maximum absolute values of all of the regulated outputs had been significantly reduced in comparison with those in the case of no control (i.e., open loop). Compared to the case of feedback-only control, the maximum absolute values of most (not all, possibly could be enhanced by using distributed control surfaces along the wing span) of the regulated outputs had been also noticeably reduced.

In the case of multi-channel fixed-structure H_∞ optimal control, it can be seen from Fig. 7 that the overall behavior with increasing preview horizon is very similar

than in the full-order case. By increasing the tuning parameter β, the H_∞ norm of the overall system increases, which, for the first impression, might be seen as a performance degradation. This is logical since the gain of the first performance channel has been increased and the second channel was kept as it was.
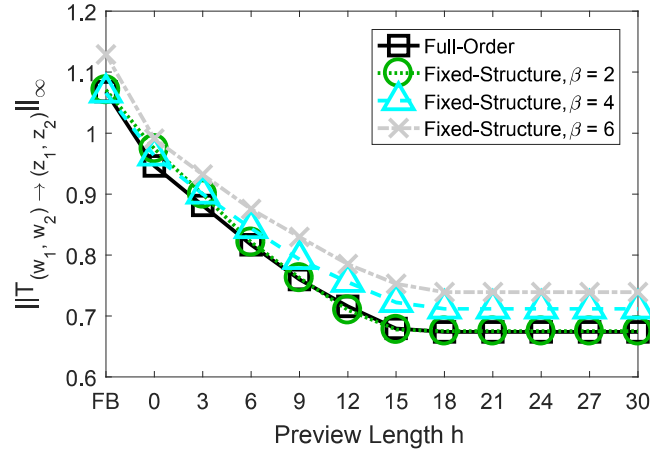

Fig. 7 H_∞ norm as function of preview length for different values of tuning parameter (FB: Feedback-only)

The multi-channel synthesis actually minimizes the maximum of both channels taken separately. The H_∞ norm of each channel (without the additional weight β on the first channel) is shown separately in Fig. 8. It can be seen that the H_∞ norm of the normal load factor at pilot location (channel 1) decreases with increasing the tuning parameter β (i.e., a performance enhancement for this specific channel). On the other hand, this comes at the expense of increasing the H_∞ norm of the structural loads (channel 2). This behavior was expected and typical for a change in relative weighting between objectives in multi-objective optimization. The evolution of the first channel norm with increasing preview length h is not monotonically decreasing in the case $\beta = 2$. The first channel in the case $h = 0$ (vertical wind available instantaneously but not in advance) has a higher H_∞ norm than in the feedback case (no wind measurement at all). The reason for that is that in both of these cases the H_∞ norms of the first channel – once multiplied with $\beta = 2$ – are still lower than the H_∞ norms of the second channel. The control design algorithm therefore fully used the additional wind information to improve the most critical criteria: the loads, i.e. the performance of the second channel.

These results are confirmed by the peak values obtained from time domain simulations. For each controller a gust encounter was simulated and the maximum absolute values (over time) of the various loads, of the load factor at pilot's location, and of the control surface deflections are shown in Fig. 9. On this figure, the trade-off between the pilot load factor and the loads can also be well observed. It should also
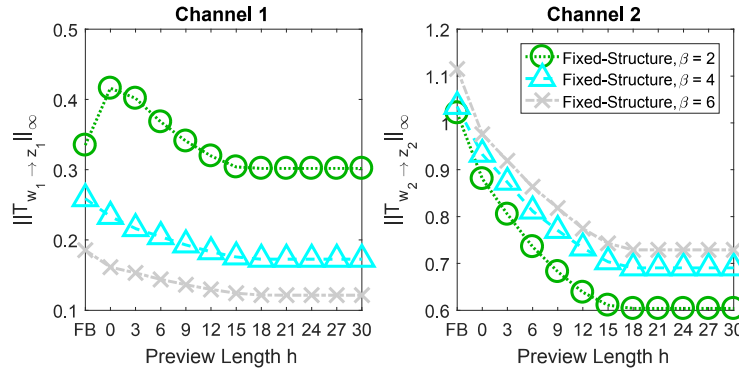
Fig. 8 H_∞ norm of each channel as function of preview length for different values of tuning parameter (FB: Feedback-only, Channel 1: normal load factor at pilot location, Channel 2: structural loads)

be noticed that including the wind measurement (low values for *h* compared to the pure feedback case) leads to increased maximum control surface deflections. The further increase of the preview horizon length (i.e. increasing *h*) leads to loads and load factor improvements but without requiring higher control surface deflections. The general trend for the maximum control surface deflections is not very strong but seems to indicate a decrease in control surface deflections with increasing preview horizon length.

4 Conclusion

A new formulation of the control design of combined feedforward and feedback load alleviation functions based on a combination of discrete-time multi-channel H_∞ control techniques and preview control was presented. This work complements a series of previous works published by the authors as well as other researchers. The application to a relatively simple sailplane model showed the expected properties; and this very first step confirms that this control design methodology is very promising for load alleviation function design. Many improvements are foreseen and future work includes increasing the granularity of the control design criteria (probably significantly more channels), investigating the robustness properties, including roll-off criteria on the control commands (e.g. some of the gains with pure feedback or short preview horizons tend to be relatively large), as well as designing methodologies for gain scheduling over the flight envelope. This technique will also be applied to other airplanes in the near future.
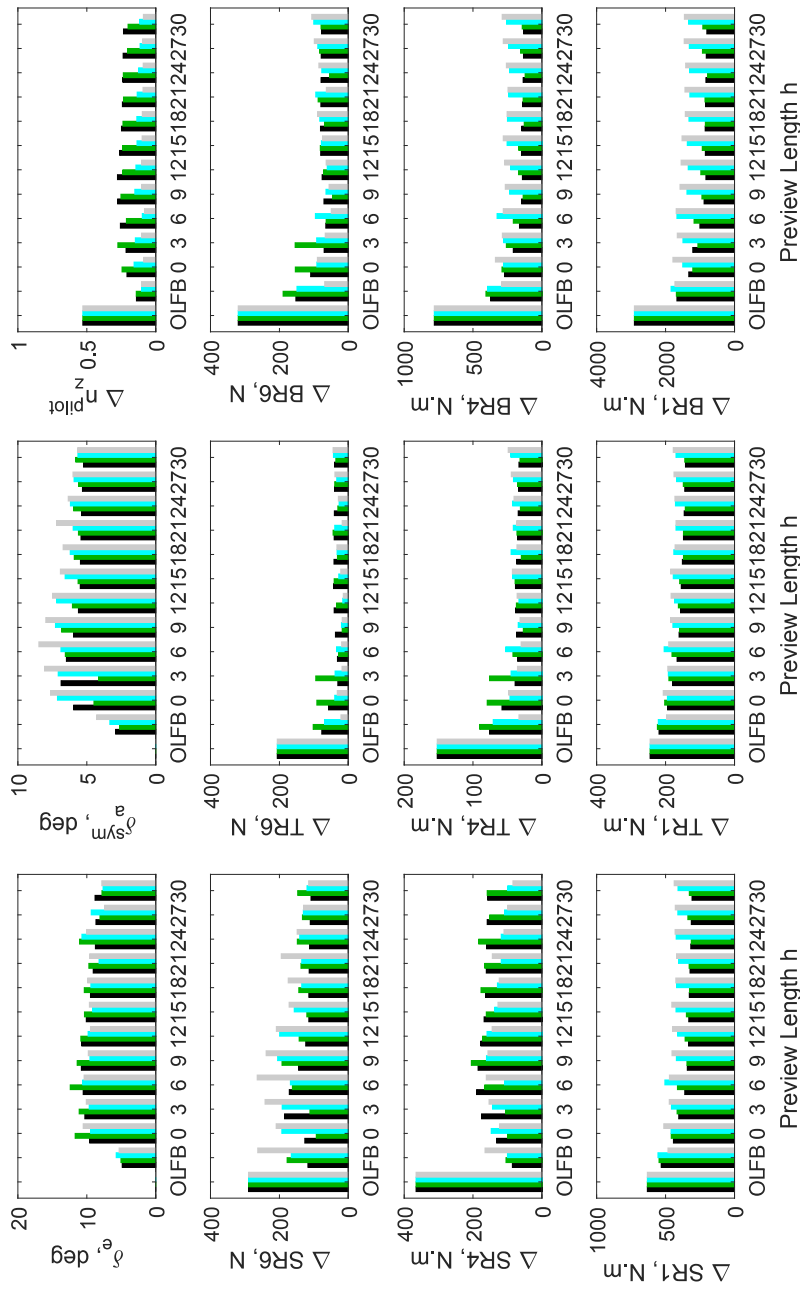
Fig. 9 Maximum absolute values of the control inputs and the regulated outputs as function of preview length for different values of tuning parameter (OL.: Open Loop, FB: Feedback-only, Black: Full-order, Green: Fixed-structure $\beta = 2$, Cyan: Fixed-structure $\beta = 4$, Gray: Fixed-structure $\beta = 6$)

5 Acknowledgments

References

1. J. Ackerman. *Robust Control - Systems with Uncertain Physical Parameters*. Springer-Verlag, 1993. ISBN 3-540-19843-1 / 0-387-19843-1.
2. P. Apkarian and D. Noll. Nonsmooth H_∞ synthesis. *IEEE Transactions on Automatic Control*, 51(1):71–86, January 2006.
3. P. Apkarian and D. Noll. Nonsmooth optimization for multidisk H_∞ synthesis. *European Journal of Control*, 12(3):229–244, May 2006.
4. N. Birla and A. Swarup. Optimal preview control: A review. *Optimal Control Applications and Methods*, 36(2):241–268, 2014.
5. P. M. Burris and M. A. Bender. Aircraft load alleviation and mode stabilization: B-52 system analysis, synthesis, and design. Technical Report AFFDL-TR-68-161, Air Force Flight Dynamics Laboratory AFFDL, November 1969.
6. J. C. Doyle, K. Glover, P. P. Khargonekar, and B. A. Francis. State-space solutions to standard H_2 and H_∞ control problems. *IEEE Transactions on Automatic Control*, 34(8):831–847, August 1989.
7. B. Etkin and D. R. Lloyd. *Dynamics of Flight: Stability and Control*. Wiley, NY, USA, 3 edition, 1996.
8. N. Fezans. An unusual structure for a feedforward gust load alleviation controller. In *Proceedings of the 2017 CEAS EuroGNC Conference*, Warsaw, Poland, April 2017.
9. N. Fezans and H.-D. Joos. Combined feedback and LIDAR-based feedforward active load alleviation. In *AIAA Atmospheric Flight Mechanics Conference*, AIAA AVIATION Forum, (AIAA 2017-3548), Denver, CO, USA, 2017. AIAA.
10. N. Fezans, H.-D. Joos, and C. Deiler. Gust load alleviation for a long-range aircraft withand without anticipation. *CEAS Aeronautical Journal*, 2019. DOI: 10.1007/s13272-019-00362-9.
11. N. Fezans, J. Schwithal, and D. Fischenberg. In-flight remote sensing and identification of gusts, turbulence, and wake vortices using a Doppler LIDAR. *CEAS Aeronautical Journal*, 8(2), June 2017. doi:10.1007/s13272-017-0240-9.
12. P. Gahinet and P. Apkarian. A linear matrix inequality approach to H_∞ control. *Robust and Nonlinear Control*, 4(4):421–448, 1994.
13. J. Herbst and P. Vrancken. Design of a monolithic Michelson interferometer for fringe imaging in a near-field, UV, direct-detection Doppler wind lidar. *Applied Optics*, 55(25):6910–6929, September 2016.

14. A. Khalil. Flight dynamics, handling and ride qualities of a flexible aircraft. In *German Aerospace Congress (Deutscher Luft- und Raumfahrtkongress / DLRK)*, Munich, Germany, September 2017. DGLR.

15. A. Khalil and N. Fezans. Performance enhancement of gust load alleviation systems for flexible aircraft using H_∞ optimal control with preview. In *AIAA Atmospheric Flight Mechanics Conference*, San Diego, CA, USA, 2019. AIAA-2019-0822. https://doi.org/10.2514/6.2019-0822.

16. H. K. Khalil. *Nonlinear Systems*. Prentice-Hall, 3rd edition, 2002. ISBN: 0-13-067389-7.

17. A. Kojima and S. Ishijima. H_∞ performance of preview control systems. *Automatica*, 39:693–701, 2003.

18. A. Kojima and S. Ishijima. H_∞ preview tracking in output feedback setting. *Robust and Nonlinear Control*, 14(7):627–641, May 2004.

19. R. H. Moroto, R. R. Bitmead, and B. Sleegers. The information structure of feedforward/preview control using forecast data. In *19th IFAC World Congress*, Cape Town, South Africa, 2014.

20. D. Ossmann and C. Poussot-Vassal. Minimal order disturbance estimator design for aircraft load alleviation control. In *2nd IEEE Conference on Control Technology and Applications*, Copenhagen, Denmark, 2018.

21. D. Ossmann and C. Poussot-Vassal. Design and assessment of a two degree of freedom gust load alleviation system. In *5th CEAS Conference on Guidance, Navigation, and Control*, Milan, Italy, 2019.

22. G. J. Rabadan, N. P. Schmitt, T. Pistner, and W. Rehm. Airborne lidar for automatic feedforward control of turbulent in-flight phenomena. *Journal of Aircraft*, 47(2):392–403, March-April 2010.

23. C. D. Regan and C. V. Jutte. Survey of applications of active control technology for gust alleviation and new challenges for lighter-weight aircraft. Technical Report NASA/TM-2012-216008, DFRC-E-DAA-TN4736, NASA, April 2012.

24. D. Schmidt. *Modern Flight Dynamics*. McGraw-Hill Education, NY, USA, 1 edition, 2012.

25. K. Takaba. A tutorial on preview control systems. In *IEEE SICE 2003 Annual Conference*, Fukui, Japan, 2003. IEEE.

26. M. V. P. Viana. *Multipoint Model for Flexible Aircraft Loads Monitoring in Real Time*. PhD thesis, Technical University of Braunschweig, Braunschweig, Germany, 2016. ISSN: 1434-8454, ISRN: DLR-FB–2016-66.

27. M. V. P. Viana. Time-domain system identification of rigid-body multipoint loads model. In *AIAA Atmospheric Flight Mechanics Conference*, AIAA AVIATION Forum, (AIAA 2016-3706), Washington, DC, USA, 2016. AIAA. DOI: 10.2514/6.2016-3706.

28. E. Zattoni. H_2-optimal rejection with preview: Geometric constraints and dynamic feedforward solutions via spectral factorization. *Kybernetika*, 44(1):3–16, 2008.

29. K. Zhou, J. C. Doyle, and K. Glover. *Robust and optimal control*. Prentice Hall, 1996.